

Imaging assessment of profound sensorineural deafness with inner ear anatomical abnormalities

Wei-Jing Wu^{a,1}, Xiang-Bo He^{a,1}, Li-Hua Tan^b, Peng Hu^a, An-Quan Peng^a, Zi-An Xiao^a,
Shu Yang^a, Tian Wang^{a,c}, Jie Qing^a, Xin Chen^a, Jing-Kun Li^a, Tao Peng^a, Yun-Peng Dong^a,
Xue-Zhong Liu^{a,d}, Ding-Hua Xie^{a,*}

^a Department of Otolaryngology and Head & Neck Surgery, Institute of Otology, Second Xiangya Hospital, Central South University, Changsha, Hunan, 410011, China

^b Department of Radiology, Second Xiangya Hospital, Central South University, Changsha, Hunan, 410011, China

^c Departments of Otolaryngology-Head and Neck Surgery, Stanford University School of Medicine, Stanford, CA, 94305, USA

^d Departments of Otolaryngology-Head and Neck Surgery, Leonard M. Miller School of Medicine, University of Miami, Miami, FL, 33101, USA

Received 11 January 2014; revised 17 January 2014; accepted 25 January 2015

Abstract

Objective: To explore the value of a combined computed tomography (CT) and magnetic resonance imaging (MRI) in evaluating profound sensorineural deafness patients before cochlear implant (CI) surgery.

Methods: A retrospective analysis of 1012 cases of profound sensorineural deafness that received CI was performed.

Results: A total of 96 cases were diagnosed with inner ear abnormalities including large vestibular aqueduct syndrome (LVAS, n = 61), Michel deformity (n = 3), cochlear incomplete partition I (n = 2), cochlear incomplete partition II (n = 6), cochlear hypoplasia with vestibular malformation (n = 3), cochlear ossification (n = 3), bilateral internal auditory canal obstruction (n = 5) and internal auditory canal stenosis (n = 2).

Conclusion: High resolution CT (HRCT) can display bony structures while MRI can image the membranous labyrinth in preoperative evaluation for cochlear implantation. The combination of these two modalities provides reliable anatomical information regarding the bony and membranous labyrinths, as well as the auditory nerve.

Copyright © 2015, PLA General Hospital Department of Otolaryngology Head and Neck Surgery. Production and hosting by Elsevier (Singapore) Pte Ltd. This is an open access article under the CC BY-NC-ND license (<http://creativecommons.org/licenses/by-nc-nd/4.0/>).

Keywords: Cochlea; Hearing loss; Multimodal imaging

1. Introduction

Cochlear implant (CI) is the primary method to restore hearing in patients with severe sensorineural hearing loss. In China, increasing number of patients achieve satisfactory hearing restoration and speech and spoken language skills through CI surgery. Experience and studies show that strict and comprehensive candidate selection, improved surgical skills, effective rehabilitation training and post-implantation psychotherapy are important for the success of CI. Contraindications to cochlear implantation may include a defect of the

* Corresponding author. Department of Otolaryngology and Head & Neck surgery, and Institute of Otology, Second Xiangya Hospital, Central South University, 139 Renmin Road, Changsha, Hunan, 410011, China. Fax: +86 731 85606003.

E-mail address: dhuaxie@163.com (D.-H. Xie).

Peer review under responsibility of PLA General Hospital Department of Otolaryngology Head and Neck Surgery.

¹ The first two authors contributed equally to this paper.

auditory nerve, and deafness caused by a severe cochlear malformation, although some cases of inner ear anomalies can achieve satisfactory outcomes. To ensure the success of CI surgery, complete preoperative evaluation should include imaging studies for temporal bone anatomy and the auditory nerve pathway. High resolution computed tomography (HRCT) can clearly reveal the anatomy of the mastoid, outer ear, middle ear, inner ear, bony labyrinth, and internal auditory meatus. Moreover, magnetic resonance imaging (MRI) allows evaluation of the auditory nerve, brain and auditory center, in addition to detecting the bony labyrinth and its pathological changes. Comprehensive evaluation of imaging studies is of important significance in determining the suitable ear for CI, evaluating electrode placement, and predicting intraoperative and postoperative complications (Li et al., 2006). In this paper, we analyze pre-operative imaging before CI surgery from November in 2005 to April in 2014 in our hospital and discuss the value of combined computed tomography (CT) and MRI in evaluating profound sensorineural deafness patients before CI surgery.

2. Materials and methods

2.1. Clinic data

We included 1012 patients with profound sensorineural deafness who received CI at the 2nd XiangYa Hospital of Central South University between November 2005 and April 2014 (the research group). Inclusion criteria included auditory examination showing bilateral profound sensorineural deafness (PTA >90 dB HL); age ≥ 12 months; no significant improvement in hearing and speech after hearing rehabilitation training for 3–6 months and meeting the conditions of hearing and speech rehabilitation training; parents and family members having a strong desire to improve patient's hearing and holding realistic expectations of CI. All the subjects and their family members agreed to partake in this research and signed the informed consent form.

2.2. Imaging examination method

All the children in the research and control group received HRCT scan and MRI examination. A 64-slice and dual-source layer 256 spiral CT scanner was used for CT scans. Patients took a supine position, with the chin tucked and the orbit line kept parallel with scan baseline. The entire structures of both middle and inner ears were included in the scan range. Volume data were collected to reconstruct cross-sectional, coronal and sagittal plane images and combined with volume rendering technology to show bony labyrinth. Pneumatization of mastoid, the size of sigmoid sinus and jugular fossa, cochlear niche, development of cochlea and internal auditory canal were examined separately. Meanwhile, the length and width of mastoid were measured. We measured the diameter of vestibular aqueduct at its external aperture and midpoint of a line connecting the posterior and anterior semicircular canals. The scan parameters were: 120 kV, 100 mA, beam collimation 0.75 mm, Pitch 1 and FOV 100 mm. We also reconstructed the

ear with 0.1 mm reconstruction interval and 50 mm FOV overlapping amplification reconstruction.

A GE Twin speed 1.5T superconducting MRI scanner was used for MRI scan. Children who could not cooperate were given 0.5 mg chloral hydrate per kilogram body weight orally or per rectum for sedation. Head scan was performed conventionally. Inner ear and auditory nerve scans were performed twice using FIESTA sequence on standard axial views and the parameters were TR 12.25 ms, TE 59.0 ms, Flip angle 700, effective slice thickness 0.6 mm, matrix 230×512 , vision 200 mm, that was used to observe the vestibular nerve, cochlear nerve and inner ear membranous labyrinth. To acquire auditory nerve images, MRP was performed perpendicular to the long axis of the internal auditory canal.

Referring to the classification criteria of inner ear malformations by Sennaroglu, diagnosis standards were established and inner ear malformations were divided into cochlear malformation, vestibular malformations, semicircular canal malformation, malformation of internal auditory canal, vestibular aqueduct malformations and cochlear aqueduct deformity. Among these malformations, cochlear malformation was divided into Michel deformity, cochlear aplasia, common cavity, cochlear hypoplasia, incomplete partition I and incomplete partition II, also known as Mondini dysplasia.

2.3. Imaging analysis of cochlear translocation malformation

2.3.1. Case groups

(1) Normal controls: temporal bone CT scan from 20 children (40 ears) with normal hearing; (2) Normal cochlear position group: axial temporal bone CT scans before CI surgery from 20 children (40 ears) with bilateral profound sensorineural deafness, who matched the inclusion criteria; (3) Abnormal cochlear position group: axial temporal bone CT scans from three 1–3 years old children whose cochleae could not be successfully accessed from the normal position during the CI surgery.

2.3.2. Measuring method

Each case was measured as follows: (1) the angle between cochlear basal turn plane and head midsagittal plane (α) (Fig. 1A), (2) the angle between a line connecting the midpoint of the facial nerve vertical section and the upper edge of the round window niche and head midsagittal plane (β) (Fig. 1B), (3) in the round window plane, the vertical distance from the surface of facial nerve vertical section to the external canal wall (Fig. 1C).

In addition, we also evaluated cochlear ossification and fibrosis that could affect CI through radiography.

3. Results and analysis

3.1. Absence of inner ear abnormalities in majority of cases

HRCT and MRI results showed normal inner ear structures in 916 of the 1012 cases, with clear imaging of the cochlea,

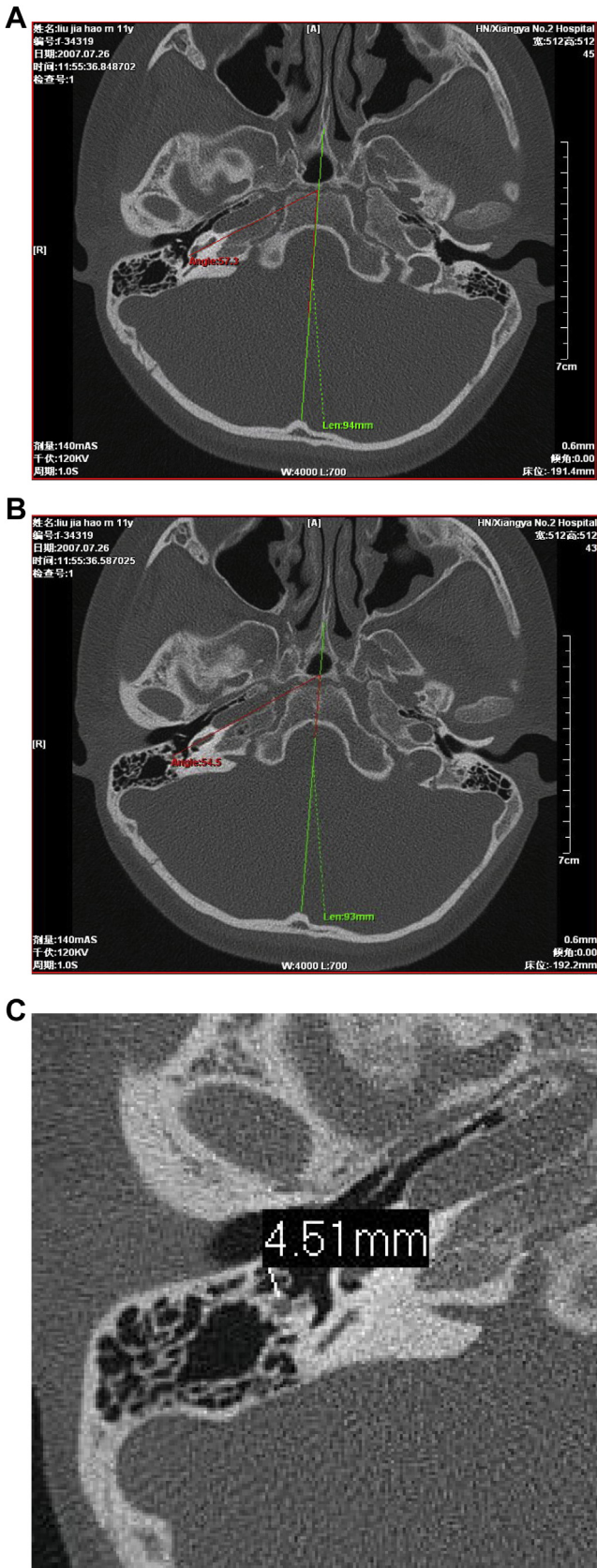


Fig. 1. Imaging analysis of cochlear translocation malformation. A: The angle between cochlear basal turn plane and head midsagittal plane (red lines). B: The angle between a connection line from facial nerve vertical section midpoint to the upper edge of the round window niche and head midsagittal

vestibular window, cochlear window and normal development of the internal auditory canal on HRCT and corresponding MRI results with no abnormal radiological changes in the cochlea, vestibule and internal auditory canal. Also, there was no apparent abnormality in the facial nerve from the brainstem to the internal auditory canal, the cochlear nerve or the vestibular nerve. MRI clearly showed cochlear patency and the development of cochlear nerve.

3.2. Imaging findings of large vestibular aqueduct syndrome (LVAS)

CT examination from 61 cases revealed cone or trumpet-shaped enlarged vestibular aqueduct bilaterally with sharp edges (Fig. 2A). MRI showed that all the patients with LVAS had unilateral or bilateral expansion of the endolymphatic sac, as a pouch pocket, flat oval or bar or curved protrusion on the surface of the cerebellum laterally posterior to the internal auditory canal with clear and smooth borders and high signals (Fig. 2B).

3.3. Michel deformity

In the research group, we found 3 cases of Michel deformity. HRCT studies: structures of bilateral cochlea, vestibules and lateral semicircular canals were not clear and showed only an ovoid cystic cavity (Fig. 3A). MRI studies: on axial, coronal, and sagittal T1W, T2W scans, imaging showed bilateral cochleae, vestibules and lateral semicircular canals forming an oval structure. Meanwhile, the normal morphological development of the brain, the internal auditory canal, and the cochlear nerve was absent (Fig. 3B).

3.4. Imaging findings in cochlear incomplete partition I

Two cases of cochlear incomplete partition I were found in the research group. CT scans showed that the actual size of the cochlea was normal bilaterally, but the interval was incomplete or absent, displaying an empty cochlear appearance. Bilateral cochlear and vestibular organs showed an abnormal cystic expansion, although outlines could still be distinguished. We also found an expansion of the vestibule, basal internal auditory canal hypoplasia and a shortened horizontal semicircular canal (Fig. 4A), but without enlarged vestibular aqueduct. MRI demonstrated that both the cochlea and the vestibule had a cystic appearance (Fig. 4).

3.5. Imaging findings of cochlear incomplete partition II (Mondini dysplasia)

We found 6 cases with cochlear incomplete partition II in the research group. This malformation showed missing

plane (green lines). C: Vertical distance A from the surface of facial nerve vertical section to the external canal wall in a round window plane.

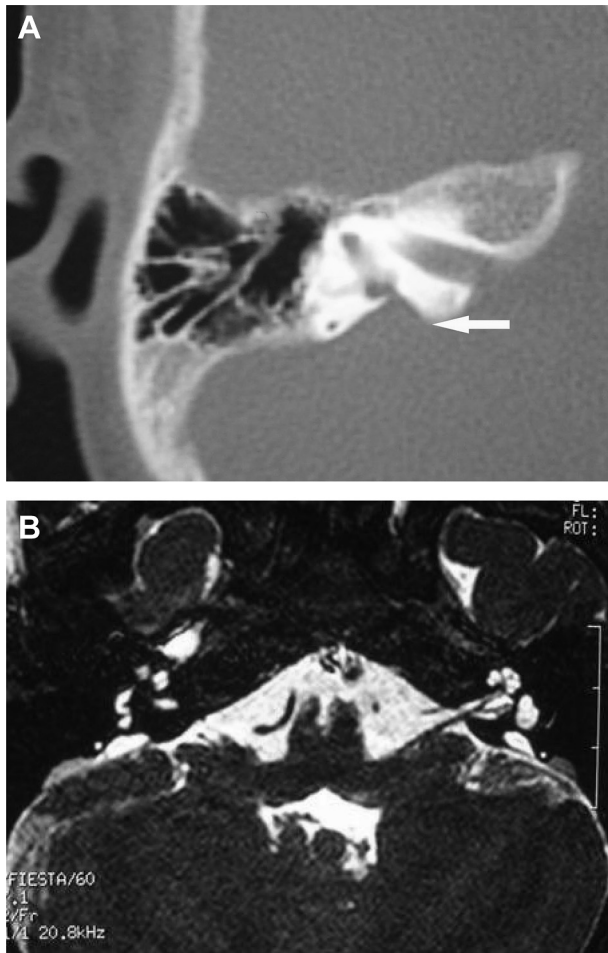


Fig. 2. Imaging findings of large vestibular aqueduct syndrome. A: CT scan images with a white arrow pointing to enlarged vestibular aqueduct. B: MRI images showing enlarged endolymphatic canal and sac.

interval bone between the middle and apical turns of the cochlea bilaterally, leading to a common space or cloaca. Instead of two and one-half turns in the bony cochlea, there were only one and one-half turns in the cochlea. Meanwhile, the length of the cochlear duct and the height of modiolus were significantly less than normal (Fig. 5A). MRI of the inner ear fluid showed a cochlea with just one and one-half turns, with the middle and apical turns forming a common space or cloaca. Due to low signals, modiolus was not clearly visible (Fig. 5B).

3.6. Cochlear hypoplasia combined with vestibular malformation

In this research group, we found 3 cases of cochlear hypoplasia combined with vestibular malformation. HRCT results suggested severe cochlear dysplasia, vestibular cavity extension, semicircular canals deformity, bony defects in the basal internal auditory canal and vestibules open to the internal auditory canal (Fig. 6A). MRI showed absence of the cochlear perilymphatic space and vestibular cavity deformity connected with the internal auditory canal (Fig. 6B).

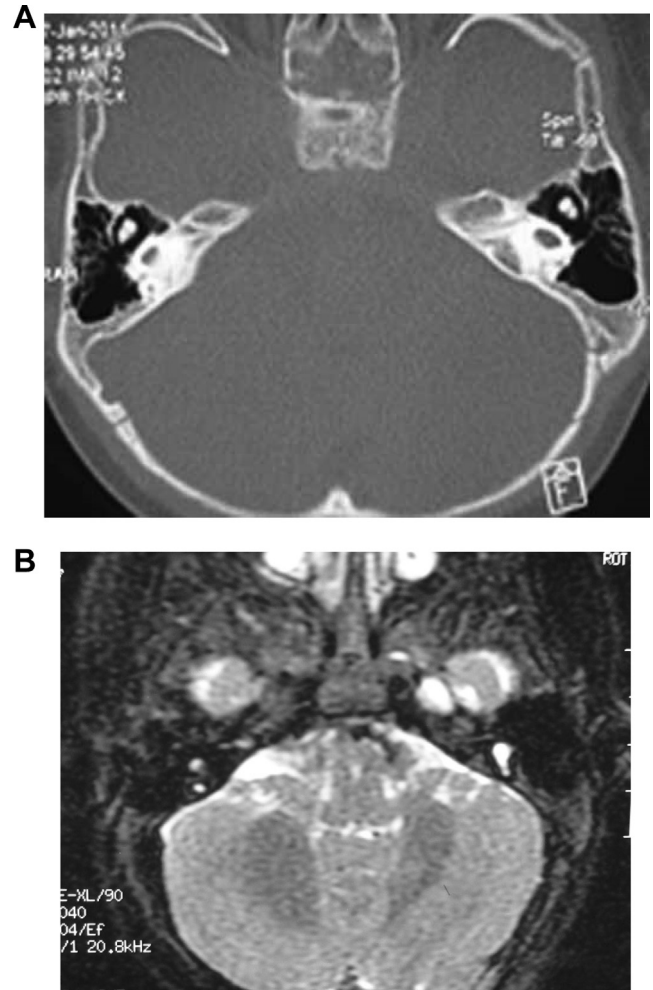


Fig. 3. Imaging findings of Michel deformity. A: CT; B: MRI.

3.7. Imaging findings of cochlear ossification

We found 3 cases of cochlear ossification in our research group. Of the 3 cases, HRCT revealed bilateral cochlear ossification in 2 patients. In one case, the severity of ossification differed between the two sides, severe on the left but mild on the right. Severe ossification in the left ear involved the entire cochlea. The density of the membranous labyrinth was significantly higher, displaying blurred edges and a slightly lower than normal bony labyrinth. Meanwhile, the structures of the modiolus and bony spiral plate appeared fuzzy with obvious narrow base and obscured border between apical and middle turns (Fig. 7). In contrast to HRCT, MRI results did not detect the presence of bilateral cochlear ossification in neither cases. In another patient, the left cochlea was not visible but perilymph cavity was visible in the right cochlea.

3.8. Imaging findings of internal auditory canal abnormalities

We found 5 patients with bilateral internal auditory canal obstruction associated with cochlear nerve dysplasia and 2

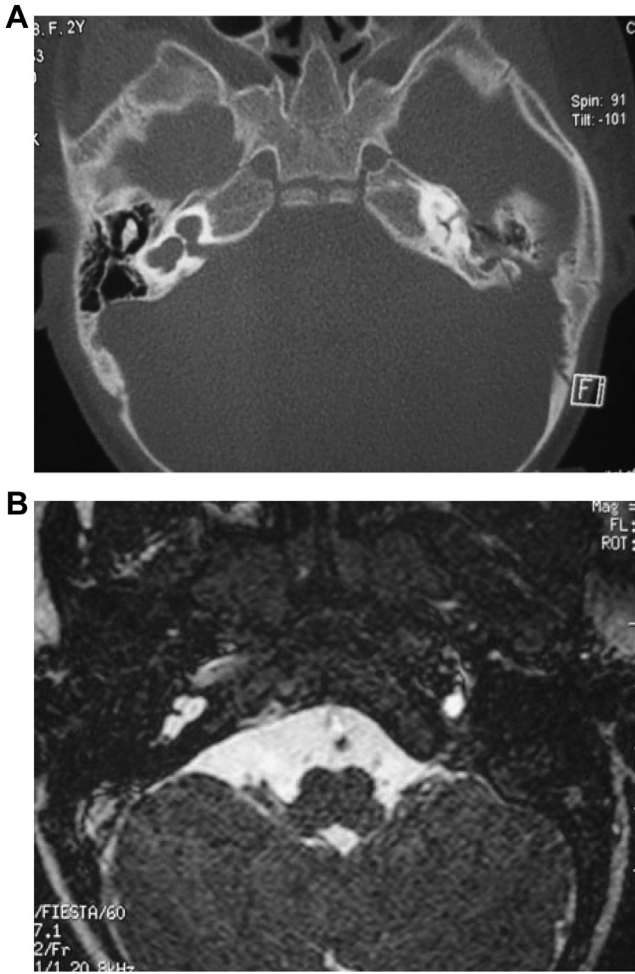


Fig. 4. Imaging findings of cochlear incomplete partition I. A: CT; B: MRI.

cases with right internal auditory canal stenosis. Cross-sectional CT showed that internal auditory canal was severely narrowed, the anteroposterior and vertical diameters were clearly minimal and the width of the opening was only 1 mm (Fig. 8A); Cross-sectional and coronal T2WI MRI showed high signal intensity in the internal auditory canal, indicative of cerebrospinal fluid (CSF). 3D-CISS imaging confirmed the absence of the cochlear and vestibular nerves (Fig. 8B).

3.9. Image analysis results of cochlear translocation malformation

In control groups, angles α and β and mean distance A were $60.5 \pm 3.6^\circ$, $48.5 \pm 6.7^\circ$ and 4.49 ± 0.37 mm, respectively. There were no significant differences between the normal control and the normal cochlear position groups ($P < 0.05$). Compared to the normal control and normal cochlear position groups, α and distance A in the 3 cases in the abnormal cochlear position group were not statistically different, although β was greater than in the other two groups. β in the 3 cases were beyond or near the upper limit of reference range

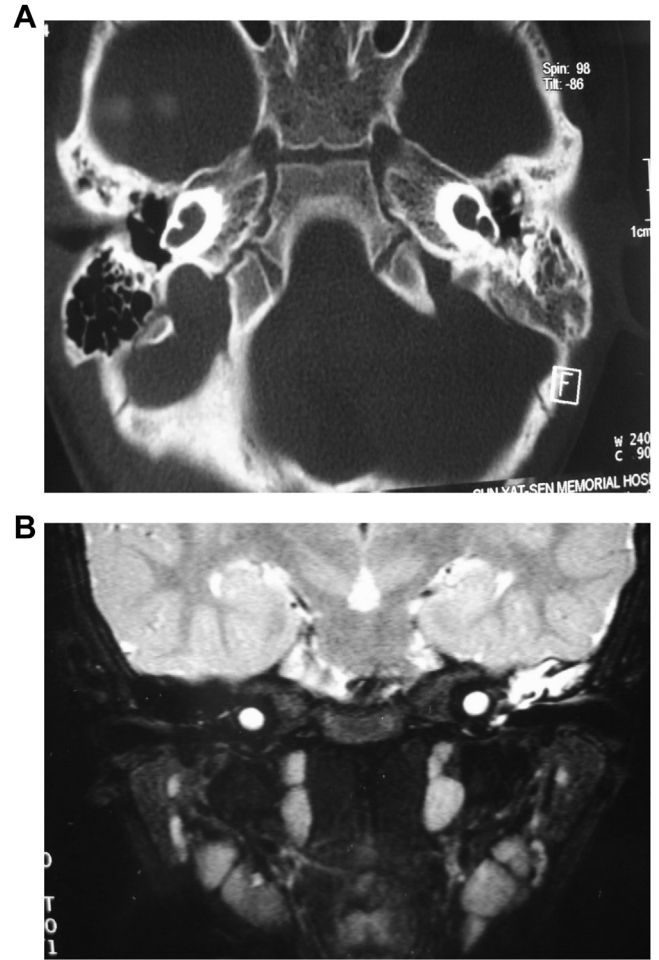


Fig. 5. Imaging findings of Mondini dysplasia. A: CT; B: MRI.

bilaterally. In the abnormal cochlear position group, α was smaller than β (Fig. 9A). In contrast, in the control groups, α was greater than β (Fig. 9B).

4. Discussion

Congenital sensorineural deafness is mainly due to developmental abnormalities of the inner ear, especially the cochlea. However, the occurrence of any lesions in the auditory pathway, including the cochlear nerve, can cause deafness. The most effective treatment for profound sensorineural deafness is cochlear implantation. Therefore, determining the site of the lesion through preoperative examination is required to formulate the best approach for cochlear implantation surgery, and to achieve optimal results of rehabilitation. Imaging analysis is one of the most important preoperative assessment instruments.

Cochlear abnormalities, caused by a variety of congenital malformations in the inner ear, and acquired diseases may affect the efficacy of cochlear implant surgery. According to the literature, the incidence of inner ear malformation is approximately 20% in patients with severe sensorineural deafness (van Wermeskerken et al., 2007). The inner ear

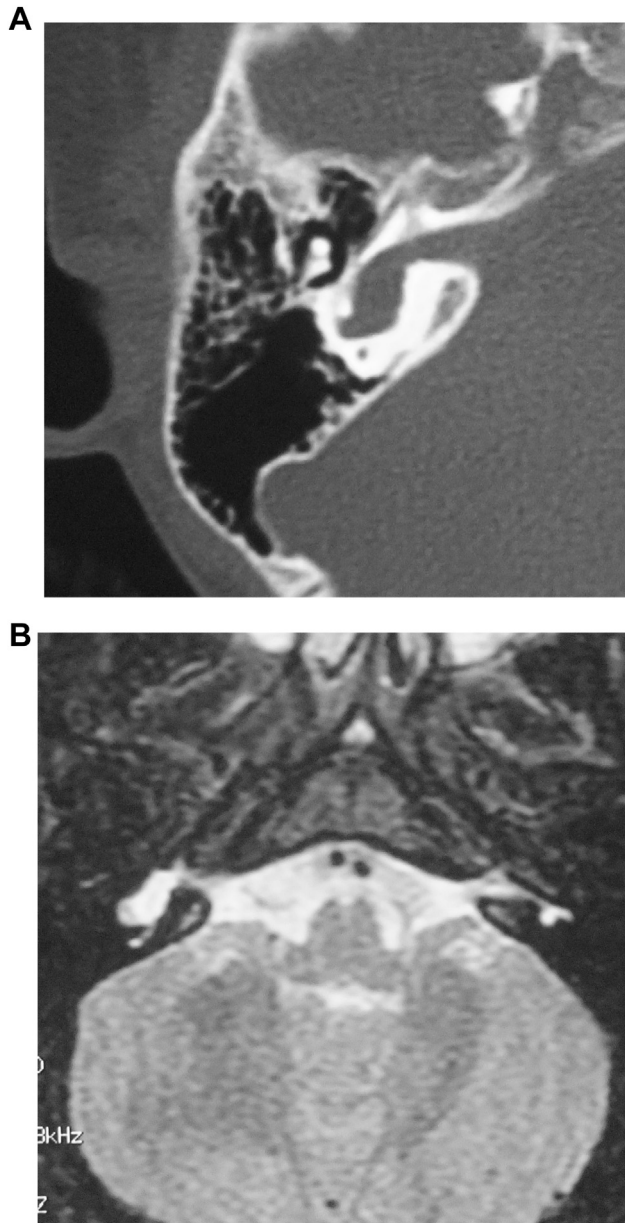


Fig. 6. Cochlear hypoplasia combined vestibular malformation. A: HRCT showing undeveloped cochlea, vestibular deformity combined with internal auditory canal. B: MRI showing the vestibule connected with internal auditory canal, and absence of cochlear perilymphatic space.

primordium is the derivative of the auditory placode arising from the ectoderm. Inner ear malformations can involve the vestibule, semicircular canals, cochlea, endolymphatic sac and vestibular aqueduct. These malformations occur in the auditory vesicle, and malformations in the internal auditory tract are from non-auditory vesicle. Genetic factors, chromosomal aberrations, congenital infection or exposure to certain medications at an early embryonic age, and other unknown reasons can cause the development of inner ear disorders. At present, large vestibular aqueduct syndrome is one of the inner ear malformations largely caused by genetic factors. Viral infections (such as rubella, measles, and mumps virus) and drugs (such as streptomycin, kanamycin, Miltown, thalidomide and

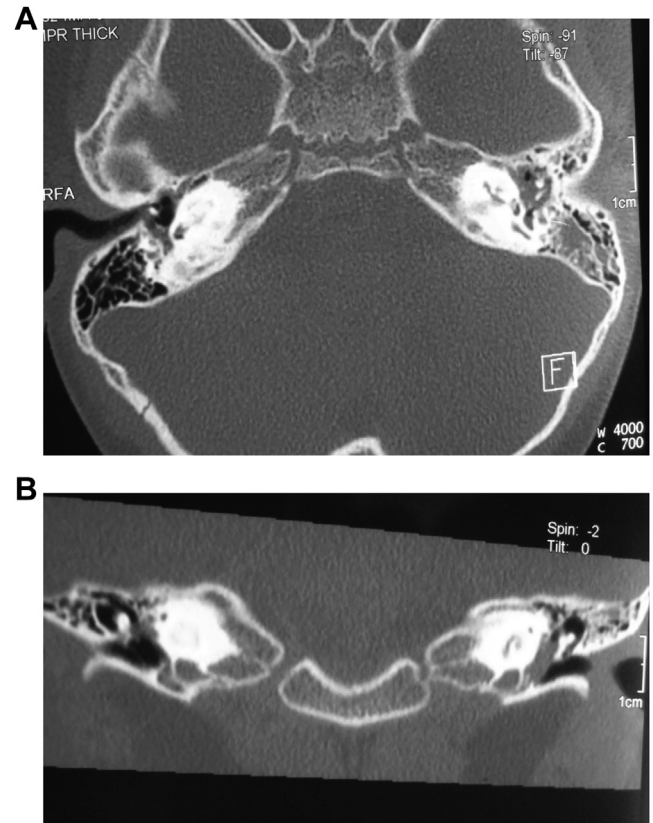


Fig. 7. CT images of cochlear ossification. A: Axial view; B: Coronal view.

so on) have been known to lead to inner ear malformations. Depending on the embryonic period when an offense occurs, different inner ear malformations may occur. Inner ear malformations can occur in any part of the bony and membranous labyrinth. Approximately 20% are bony labyrinth deformities and about 80% are membranous labyrinth malformation (Jackler et al., 1987a). The development of embryonic bony labyrinth occurs around 4–8 weeks gestation and the maturation of the membranous labyrinth occurs from 8 to 24 weeks. Therefore, bony labyrinth deformities often accompany membranous labyrinth malformations. Bony labyrinth deformities can be diagnosed by imaging examinations (Schuknecht and Gulya, 1986), but most membranous labyrinth malformation such as Scheibe and Alexander deformities cannot be seen on imaging at this time (Harnsberger, 2003).

In the past, the classification of congenital inner ear malformations, proposed by Jackler et al. (1987b) in 1987, was most widely used. He divided bony labyrinth deformities into: labyrinth deficiency (Michel deformity), cochlear aplasia, cochlear hypoplasia, incomplete partition (Mondini dysplasia) and common cavity. At that time, temporal bone imaging was mainly taken via multi-track tomography. With the advances in imaging technology, Sennaroglu proposed a new classification based on CT findings and subdivided inner ear malformation into cochlear malformation, vestibular deformity, semicircular canal deformity, internal auditory meatus deformity, vestibular aqueduct deformity and cochlear aqueduct malformation. Cochlear malformation was further divided



Fig. 8. Image findings of internal auditory canal obstruction associated with cochlear nerve dysplasia. A: CT scans showing internal auditory canal stenosis. B: axial section MRI images of internal auditory canal showing cochlear nerve aplasia.

into: (1) Michel deformity: the most severe inner ear malformation characterized by complete loss of inner ear structure. This deformity correlates to arrested development in the 3rd week of gestation. (2) Cochlear aplasia, i.e. absence of the cochlea, with the vestibule being normal, expanded or showing hypoplasia. It is also caused by arrested development at the end of the 3rd week of gestation. (3) Common cavity: cochlear and vestibular structures showing a cystic structure and indistinguishable from each other because development is halted in the 4th week of gestation. (4) Cochlear hypoplasia: cochlear and vestibular structures indistinguishable from each other, with the structure being smaller than normal. The cochlea often appears as a bud-shaped structure expanding from the internal auditory meatus. This malformation is caused by arrest of development in the 6th week of gestation. (5) Incomplete partition I: cochlea showing a sack-like structure without integral modiolus and ethmoid, usually associated with cystic dilated vestibule. This is due to the stop of development in the 5th week of gestation. (6) Incomplete partition II (also known as Mondini dysplasia): caused by a

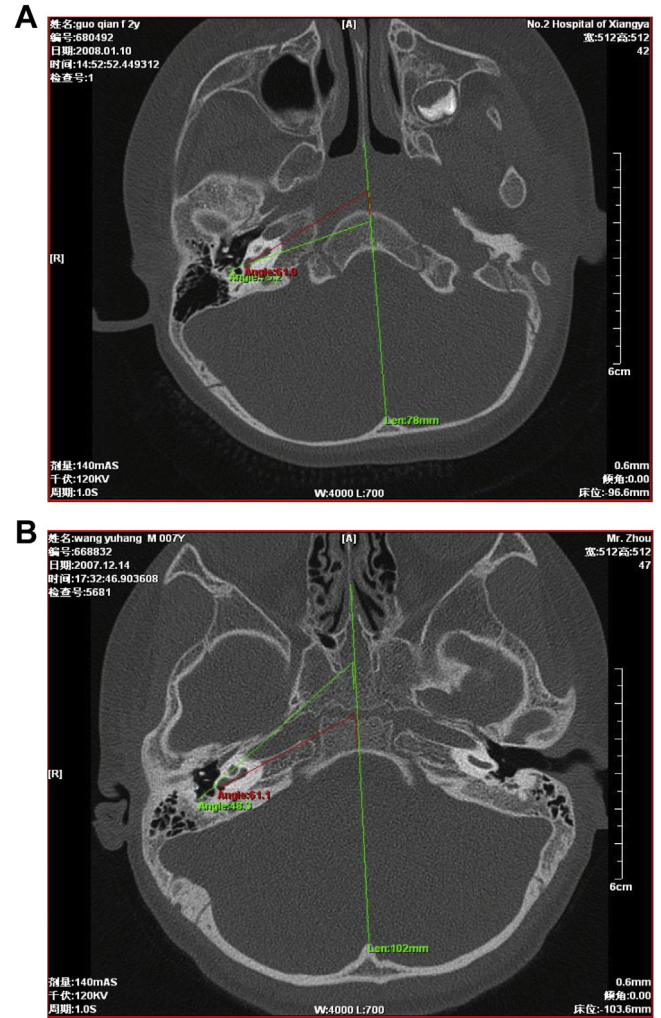


Fig. 9. α and β angles comparison between normal and cochlear translocation malformation patients. A: Cochlear translocation malformation. B: Normal cochlea.

development arrest in the 7th week of gestation, this malformation usually occurs with an enlarged vestibular aqueduct and vestibule. The cochlea has one and a half coils, and only the basal turn is normal whereas apical and middle turns merge together. Vestibular deformity and semicircular canal deformity are common. The cochlea may be normal, but there is an expansion of the vestibule and a short, thick or absent semicircular canal. Vestibular aqueduct malformations: enlarged vestibular aqueduct is one of the most common types of deformity, which is bell-mouthed or connected with common crus. Internal auditory meatus deformity: internal auditory canal stenosis, absence or expansion. Cochlear aqueduct malformations: enlarged or narrowed cochlear aqueduct is the main feature.

During CI surgery in a patient with inner ear malformation, the greatest concern is the location of the facial nerve, as well as whether there is a defect in the lateral wall of the internal auditory canal and during the course of the auditory nerve. The auditory vesicle of inner ear primordium and the Reichert cartilage of the second branchial arch formed the facial nerve

canal. Therefore, inner ear malformations can cause abnormal positions of the facial nerve canal. On the other hand, the defect of the lateral wall of the internal auditory can lead to cerebrospinal fluid connected with the lymph of the cochlea. Because of the high pressure of the cerebrospinal fluid, cerebrospinal fluid “gush” phenomenon often occurs during the surgery. Imaging studies can aid an otolaryngologist in deciding the appropriate surgical approach and reducing complications.

In displaying inner ear abnormalities, CT and MRI have their own advantages and disadvantages (Xian et al., 1999; Zhu et al., 1995). High-resolution CT provides good spatial resolution through the thin layer, small field of view, large matrix and bone algorithm. Temporal bone HRCT is generally set at 1–2 mm layers and scanned with continuous or partially overlapping technology. Bilateral scanning is routinely performed and sometimes with partial reconstruction and amplification, if necessary. Application of window technique is very important for showing different middle and inner ear structures. Generally, window width is about 4000 Hu and window level is around 400–1000 Hu. From various scan thickness and calculation methods for image reconstruction, HRCT can significantly increase the display resolution of structures including the ossicular chain and bony labyrinth compared to regular CT, which provides a basis for the accurate measurement of certain structures, diagnosis and surgery design. Meanwhile, HRCT also helps identify the development situation of inner ear bony labyrinth, including each turn of the cochlea, the degree of ossification, the development of the internal auditory canal, and the expansion of vestibule and vestibular aqueduct.

MRI technology provides better soft tissue resolution. Especially in recent years, the application of water imaging technology makes intuitive, three-dimensional display of the fine structure of the inner ear membranous labyrinth possible, compensating deficiencies of CT examination. MRI is capable of showing inner chambers containing fluid within the bony labyrinth. Furthermore, MRI three-dimensional MIP image more vividly reflects inner ear structural details, especially regarding semicircular canals morphology and their three-dimensional relationship. For cases with cochlear ossification, it is difficult to see ossification and fibrosis lesions within the membranous labyrinth on HRCT, whereas MRI can show the lesion as local low density. This proves that MRI has more advantages when studying the membranous labyrinth, the endolymph and the cochlear and vestibular nerves in the internal auditory canal. In addition, direct scanning with HRCT is limited to cross-sectional and coronal planes, but less so on sagittal or other tilted angle planes. Therefore, display of some structures is less satisfactory compared to MRI, which has its advantages in this regard.

In this study, the most common inner ear malformation was large vestibular aqueduct syndrome, which accounted for 63.5% of inner ear malformations (61/96) in this series. In our experience, CI surgery in enlarged vestibular aqueduct syndrome patients is rarely complicated by cerebrospinal fluid leakage. The characteristic finding of enlarged vestibular

aqueduct on imaging is expansion of the distal vestibular aqueduct in the endolymphatic sac region on CT. The diameter of bony vestibular aqueduct is determined by measuring the distance between the common crus and the midpoint of the outside export on axial CT images. When greater than 1.5 mm, it is considered an enlarged vestibular aqueduct. This standard was proposed by Valvassori and has been widely used (Valvassori and Clemis, 1978; Valvassori, 1983; Reussner et al., 1995). It was also used in our study for diagnosis of large vestibular aqueduct syndrome. However, a new diagnostic criterion has been suggested recently, also known as the Cincinnati criteria (Boston et al., 2007), which calls for diagnosis of enlarged vestibular aqueduct when the middle section vestibular aqueduct diameter is greater than 1.0 mm or outside diameter is greater than 2.0 mm.

The endolymphatic sac appeared enlarged on MRI in most of our patients. However, Okamoto et al. found that the size of the vestibular aqueduct on MRI did not always correspond to its actual size. Thus, Okamoto et al. believed that it was more appropriate to name this disease as “large lymphatic sac syndrome” (Okamoto et al., 1998). Under normal circumstances, the size of the endolymphatic sac is about 1 mm, and difficult to detect on MRI. Also, endolymphatic sac is hard to see in normal adults and children. Tong et al. (1997) thought that CT might show false positive or false negative results. However, MRI can clearly show the endolymphatic sac, and thus help more accurately determine whether it is in conjunction with enlarged vestibular aqueduct syndrome.

Incomplete partition II is also known as inner ear hypoplasia or Mondini dysplasia that is caused by the stop of development in the 7th week of gestation. It was first described by Mondini in 1791 and usually shows as bony labyrinth and membranous labyrinth hypoplasia that is often accompanied by middle ear abnormalities and aberrant courses of the facial nerve. Schuknecht (1980) reported the temporal bone pathology of Mondini malformation, including one and a half coils of the cochlea with only the base turn being normal and absent apical and middle turns, or the whole cochlea being a single ring. It may also include expansion of vestibular pool, endolymphatic sac and endolymphatic canal. Other abnormalities may include variation in size or absence of the semicircular canal, cochlear and vestibular receptors hypoplasia, incomplete stapedial plate in some patients, closed vestibular window, and swollen round window membrane that can lead to spontaneous rupture.

In our study, 8 patients were diagnosed with Mondini malformation through high-resolution CT and MRI of the temporal bone, and 6 of them received cochlear implantation surgery. CSF “gush” phenomenon occurred intraoperatively but cochlear electrode was implanted successfully and CSF leak repair was done at the same time. There were no facial paralysis, CSF leakage, intracranial infection, or other serious complications post-operatively.

Cochlear translocation deformity, however, can hamper cochlear implant surgery. Three were found to have cochlea backward translocation among the 1012 cases. All of them received cochlear implantation. With cochlear translocation,

the turning and the position of the promontory of cochlear basal turn is changed, making it difficult to open the window through the ordinary approach. In order to adjust to the new location of cochlear window opening and the directionality of electrode placement, attention must be paid to this deformity through preoperative detection.

Abnormal cochlear positions can be divided into cochlea translocation and cochlear shift. α (the angle between cochlear basal turn plane and head midsagittal plane) and β (the angle between a connection line from facial nerve vertical section midpoint to the upper edge of the round window niche and head midsagittal plane) measured on temporal bone CT scans can help determine whether the cochlear position is abnormal and to what degree. 95% reference range of α is 53.4° – 67.6° with the average being $60.5^{\circ} \pm 3.6^{\circ}$. 95% reference range of β is 35.4° – 61.6° with an average of $48.5^{\circ} \pm 6.7^{\circ}$. When the angle is not within the normal range, a forward or backward cochlear translocation is indicated.

Internal auditory canal malformations include absent, narrowed or dilated internal auditory canals. The normal width of the internal auditory canal is about 4–6 mm. Less than 2 mm should be considered as narrow and is usually associated with auditory nerve and/or facial nerve abnormalities. If the width is greater than 6 mm but without any clinical symptoms, it is usually not diagnosed as abnormal or expanded. For patients with internal auditory canal malformations who are being considered for cochlear implantation, attention should be focused on presence of stenosis that accounts for about 12% of congenital temporal bone deformities (Ferreira et al., 2003; Baek et al., 2003; Egelhoff et al., 1989).

The diagnosis of internal auditory canal stenosis depends on temporal bone high-resolution CT. CT can show the diameter of the internal auditory canal, but not the details inside the canal or the integrity of the auditory nerve. However, high-resolution MRI three-dimensional scanning images, combined with oblique sagittal thin layer reconstructed images perpendicular to the internal auditory canal, can clearly demonstrate the morphology of the internal auditory nerve. In our group, CT results showed <2 mm diameter of the internal auditory canal in 1 patient, and MRI also showed developmental abnormalities of the auditory nerve. However, the diameter of the internal auditory canal is not always consistent with auditory neurodevelopmental situation. Some cases have normal sized internal auditory canal, but auditory nerve hypoplasia. Therefore, for all cochlear implantation applicants, MRI examination is needed to determine auditory neurodevelopmental situation with or without internal auditory canal stenosis to ensure the efficacy of hearing rehabilitation after surgery.

Cochlear ossification and fibrosis directly affect cochlear electrode implantation. Therefore, preoperative examination is necessary to determine the patency of the cochlear cavity. However, identification of cochlear ossification may present certain degrees of difficulty. At present, the rate of diagnosis of severe cochlear ossification is up to 100% through high-resolution temporal bone CT examination, and lateral semi-circular canal ossification is the most sensitive indicator in the

diagnosis of cochlear ossification. But for cochlear fibrosis and early stage ossification, the rate of missed diagnosis remains very high (Young et al., 2000). Seidman et al. (1994) found up to 57% of misdiagnosis rate for early ossification with cochlear fibrosis on CT. Therefore, for patients with suspected cochlear ossification, additional MRI examination is necessary. Three-dimensional MR water imaging technology can show the patency of the cochlear cavity very well. As it can clearly show the outline of the structure of the membranous labyrinth and can be rotated 360° , it helps distinguish cochlear soft tissue abnormalities, cochlear fibrosis, and other internal auditory canal and retrocochlear soft tissue abnormalities that CT has failed to identify. It is therefore very helpful in selection of appropriate surgical ears (Schmidt et al., 2001).

Acknowledgments

This study was supported by the Cochlear Implantation Program of Hunan, National Basic Research Program of China (2012CB967904). We thank the patients, their families and deaf-mute school children who participated in this study.

References

- Baek, S.K., Chae, S.W., Jung, H.H., et al., 2003. Congenital internal auditory canal stenosis. *J. Laryngol. Otol.* 117, 784.
- Boston, M., Halstead, M., Meinzen-Derr, J., et al., 2007. The large vestibular aqueduct: a new definition based on audiologic and computed tomography correlation. *Otolaryngol. Head Neck Surg.* 136, 972–977.
- Egelhoff, J.C., Ball, W.S., Towbin, R.B., et al., 1989. Dural ectasia as a cause of widening of the internal auditory canal in patients with neurofibromatosis. *Pediatr. Radiol.* 17, 79.
- Ferreira, T., Shayestehfar, B., Lufkin, R., 2003. Narrow, duplicated internal auditory canal. *Neuroradiology* 45 (5), 308–310.
- Harnsberger, 2003. *Temporal Bone Top 100 Diagnoses*, vol. 35–37. Amirsys Inc, Salt Lake City, Utah, pp. 62–70.
- Jackler, R.K., Luxford, W.M., House, W.F., 1987a. Congenital malformations of the inner ear: a classification based on embryogenesis. *Laryngoscope* 97.
- Jackler, R.K., Luxford, W.M., House, W.F., 1987b. Congenital malformations of the inner ear: a classification based on embryogenesis. *Laryngoscope* 97 (3 Pt 2 Suppl. 40), 2–14.
- Li, X.H., Zhu, M., Zhang, Z.Y., et al., 2006. High-resolution CT and MRI studies of children with congenital deafness. *J. Clin. Radiol.* 25 (10), 955–958.
- Okamoto, K., Ito, J., Furusawa, T., et al., 1998. MRI of enlarged endolymphatic sacs in the large vestibular aqueduct syndrome. *Neuroradiology* 40 (3), 167–172.
- Reussner, L.A., Dutcher, P.O., House, W.F., 1995. Large vestibular aqueduct syndrome with massive endolymphatic sacs. *Otolaryngol. Head Neck Surg.* 113 (5), 606.
- Schmidt, A.M., Weber, B.P., Becker, H., 2001. Functional magnetic resonance imaging of the auditory cortex as a diagnostic tool in cochlear implant candidates. *Neuroimaging Clin. N. Am.* 11 (2), 297–330.
- Schuknecht, H.F., 1980. Mondini dysplasia: a clinical and pathologic study. *Ann. Otol. Rhinol. Laryngol.* 89 (Suppl. 65), 1.
- Schuknecht, H.F., Gulya, A.J., 1986. *Anatomy of the Temporal Bone with Surgical Implications*. Lea and Febiger, Philadelphia.
- Seidman, D.A., Chute, P.M., Parisier, S., 1994. Temporal bone imaging for cochlear implantation. *Laryngoscope* 104, 562–565.
- Tong, K.A., Harnsberger, H.R., Dahlen, R.T., et al., 1997. Large vestibular aqueduct. *AJR* 168, 1097.

- Valvassori, G.E., 1983. The large vestibular aqueduct and associated anomalies of the inner ear. *Otolaryngol. Clin. N. Am.* 16 (1), 95–101.
- Valvassori, G., Clemis, J., 1978. The large vestibular aqueduct syndrome. *Laryngoscope* 88, 273–278.
- van Wermeskerken, G.K., Dunnebiex, E.A., van Olphen, A.F., et al., 2007. Audiological performance after cochlear implantation: a 2-year follow-up in children with inner ear malformations. *Acta Otolaryngol.* 127 (3), 252–257.
- Xian, J.F., Wang, Z.C., Yan, F., et al., 1999. Application of MRI fast spin-echo T2WI 3D reconstruction techniques in the inner ear lesions. *Chin. J. Radiol.* 33 (7), 473–476.
- Young, N.M., Hughes, C.A., Byrd, S.E., et al., 2000. Postmeningitic ossification in pediatric cochlear implantation. *Otolaryngol. Head Neck Surg.* 122, 183–188.
- Zhu, XN, Lian, NJ, Cai, ZH, et al. Clinical analysis of 102 cases inner ear congenital malformations. 1995, 30(3): 157–159.